Journal of Engineering and Applied Sciences 12 (16): 4172-4174, 2017
ISSN: 1816-949X

Utilization of Polar-Current-Shell-Based Algorithm for Surface Current Extraction from Ship Borne X-Band Nautical Radar Images

R. Durga Singh
Department of GMDSS, AMET University, Chennai, India

Abstract: In this study, the use of the polar current shell-based current reversal calculation to deliver borne X-band nautical radar pictures exhibited. After the 3D image range created by a 3D-FFT of the radar picture arrangement, the extricated scattering shell is changed over to a polar frame the "polar current shell" from which the present speed of experience dictated by joining a large sinusoidal bend fitting. The calculation connected to shipborne radar information that gathered on the East Coast of Canada. The outcomes contrasted and those getting a WaMos framework and understanding between the two shows the legitimacy of the proposed calculation.

Key words: 3D, X-band, WaMos, pictures exhibited, East Coast of Canada

INTRODUCTION

Sea surface force information is profitable for toward the ocean activities and ocean course prosperity. Not in any way like *in situ* modern estimation instruments (e.g., ADCPs) X-band marine radars can give current field information inside an area of around 3×3 km^2 enveloping the radar with high spatial and transient assurance. Young *et al.* (1985) developed the small Lest Square (LS) appropriate approach to managing focus sea surface information from a progression of marine radar pictures. Cloud connected smart gas leakage detection and safety precaution system well developed by Babuprasanth (2014). A while later, a couple of other current inversion counts were made including the improved weighted LS method by Gangeskar (2002) the iterative LS approach (Senet *et al*., 2001) and the institutionalized scalar thing (NSP) procedure (Senet *et al*., 2001). Also, to refine the execution of these inversion arranges, different changes have been made and associated (Huang and Gill, 2012). All the already said rely on upon the scrambling relationship in the Cartesian encourage system. Shen *et al*. (2014), a polar-current-shell-based count presented what's more, affirmed using reenacted radar pictures. Lowland environmental technology of seismic-sediments of Kandla Port in India is defined 1 (Veerakumar *et al*., 2017).

This study followed some research articles, A soft computing approach on ship trajectory control for marine applications (Sethuramalingam and Nagaraj, 2015) investigates an approach using artificial intelligent and sweet computing may be a likely choice. Ship recycling, an important mile stone for India (Reddy and Manoharan, 2014) reviews the current state of re-use and combine the art of technology with the demands of beneficial developments from the maritime industrial sector. PLC based automatic control for onboard ship gangway conveyor system (Veerakumar *et al*., 2017) describes leakage of ships during traverse collision on an open marine environment.

M ATERIALS AND METHODS

Current algorithm:

Algorithm: The points of interest of the polar-current shell-based calculation given by Shen *et al*. (2014). The crucial usage steps Fig. 1 include.

3D-FFT (After the radar sub-picture (128×128 pixels)): A succession of 32 pictures is increased by a smooth decreasing capacity W(n) (Komen *et al*., 1996) a 3D-FFT includes 256×256×256 focuses with zero cushioning utilized past the first sub-picture data size is applied to produce the 3D image power spectrum.

I0 (k_x, k_y, ω) (k_x, k_y are wave number along x and y-pivot, individually, ω is rakish wave recurrence). Extraction of the scattering shell given the crucial mode wave scattering relationship (Komen *et al*., 1996) from the picture range; locating an exact shell of ω_j from the image control range involves the accompanying strides; High-Pass (HP) sifting I0 (kx, ky, ω) utilizing:

$$I_1(k_x, k_y, \omega) = \begin{cases} 0, & \omega < \omega_{cut} \\ I_0(k_x, k_y, \omega) & \omega \geq \omega_{cut} \end{cases} \quad (1)$$

Clearing the conceivable impedance from low-vitality foundation to clamor spikes. For each combination of (k_{xi}, k_{yi}), i = 1, 2, ..., 256 in the wavenumber plane of the 3-D picture range there exists a segment vector along the precise recurrence hub that can be meant by I1(k_{xi}, k_{yi}, ω). If the greatest vitality of this vector is lower than a limit (= I1(k_x, k_y, ω)|max/2000 here), all information focuses

inside the vector are prohibited from further handling. Prevention of cooperative black hole attack in manet on DSR protocol using cryptographic algorithm developed by Sethuramalingam and Nagaraj (2015). This methodology can likewise lessen the quantity of emphasis for consequent strides. Distinguishing the sea wave part connected with the picture ghastly pinnacles. Effective dose reduction through ventilation scheme was designed for prototype fast breeder reactor is described by Reddy and Manoharan (2014). For a particular segment vector along the rakish recurrence pivot in the range I2 (k_{xi}, k_{yi}, ω) coming about because of Eq. 2, just a single recurrence purpose of ω_j situates on the scattering shell and this is related with sea wave segments. This ω_j is resolved given pinnacle distinguishing proof by analyzing the subordinate of each point. The efficiency of plant growth promoting rhizobacteria isolated from sand dunes of Chennai coastal area explained by Tukey (1967). On the

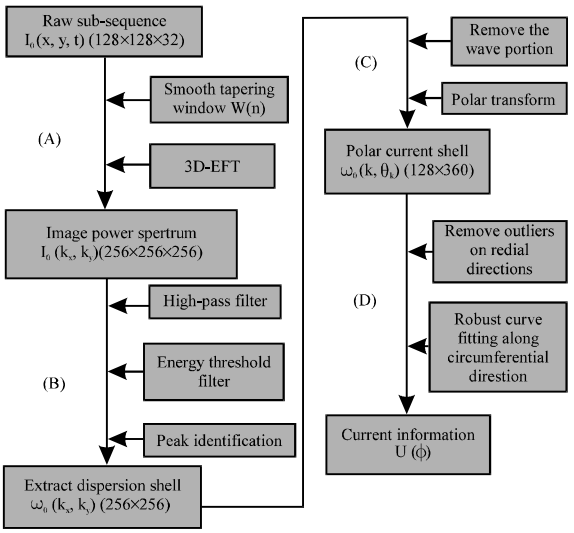

Fig. 1: Ablock diagram of the current inversion procedure (Shen *et al*., 2014) foure major steps are maked by (a-d)

off chance that just a single conspicuous pinnacle is distinguished (the paradigm here is that no other pinnacle achieves 33% the vitality of the first pinnacle) the comparing ω extricated as ω_j; generally, ω_j set to zero. In the wake of rehashing this strategy for each (k_{xi}, k_{yi}) match, a coarse scattering shell can develop from the non-zero ω_j (k_x, k_y).

Changing to current polar shell: The currently included diffusion connection might revamp as:

$$\omega U(k_x, k_y) = \vec{k} \cdot \vec{U} = kU\cos\bar{\theta} = \omega_0(k_x, k_y) - \sqrt{gk} \quad (2)$$

Deciding the present parameters: Interference because of clamor may even now fall in the current polar shell. The impedance can view as exceptions that may seriously influence the next minimum squares to fit and in this manner, must expel. As indicated by Eq. 2 for an accurate spiral bearing in the wavenumber plane, the crossing point edge θ is settled so that ωUk ought to stay steady. Along these lines, the Grubb's test is utilized to distinguish one anomaly at once and this anomaly is evacuated and the test iterated until no defects are recognized (Shen *et al*., 2014). After the impedance in every single outspread bearing is cleared, minimum squares bend fitting (Sethuramalingam and Nagaraj, 2015) along each circumferential course (i.e., for each clear sweep) is actualized utilizing the model capacity f (U, θ) = ωU k = U cosθ = U cos |θ k_ϕ_U |. It ought to notice that if the non-zero focuses inside a circumferential vector are littler than 10, the fitting procedure ought to prematurely end for this span. The point relating to the most extreme of the evaluated work f (U, θ) is resolved to be the present bearing and the adequacy of this sinusoidal capacity is the instant speed. The outcomes might arrive at the midpoint of over a band of changing the range to produce a precise current speed (Fig. 2 and 3).

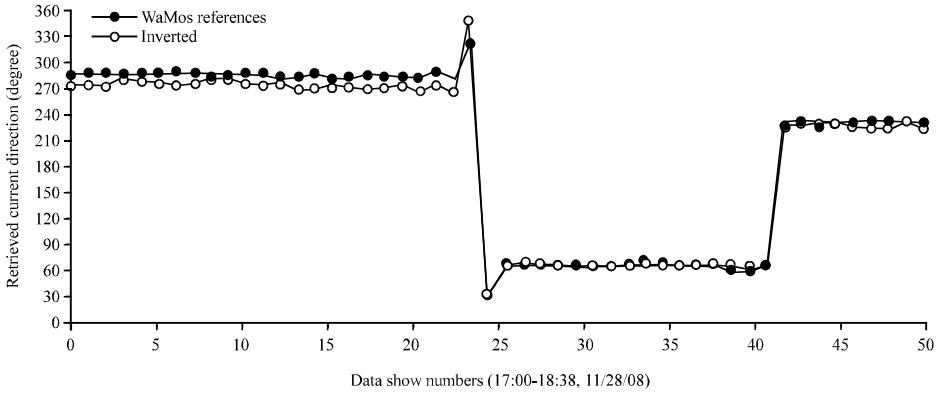

Fig. 2: Current direction extraction for the period

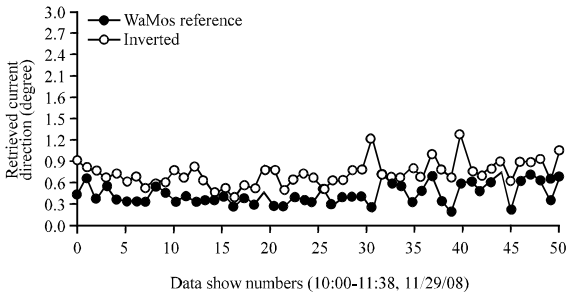

Fig. 3: Current speed extraction for the period

RESULTS AND DISCUSSION

The approval of the polar-current-shell-based calculation has been approved utilizing reproduced information by Shen *et al.* (2014). Here, further testing is executed using field information. An H-pol shipborne nautical X-band radar was mounted together with a WaMoS 2 framework by defense research and development Canada near Halifax on November 28 and 29, 2008. The radio wire worked with a turn time of figure at the time, the nearby wind speed was a negligible 5.3 m/sec and the WaMoS 2 framework likewise revealed a comparing small ocean state. Under such conditions, the SNR of the radar pictures could be low and the dependability of the reversal procedure might be fundamentally lessened (Babuprasanth, 2014). The substantial change in the WaMoS 2 comes about likewise seems to affirm this finding. By the by, great connection between's the outcomes is apparent.

CONCLUSION

In this study, the polar-current-shell-based calculation has been connected to recover current data from shipborne X-band marine radar pictures. The recovered current speeds of experience concur with the WaMos comes about because of information gathered under shifting boat movement conditions. It demonstrates that the calculation can fill in as a decent option in X-band marine radar remote detecting. Be that as it may because of the absence of ADCP current information related to the test, a free examination of the mistake measurements can't be attempted here. Additionally, testing is necessary to assess the execution of the calculation utilizing ADCP information.

REFERENCES

Babuprasanth, V., 2014. Cloud connected smart gas leakage detection and safety precaution system. Intl. J. MC. Square Sci. Res., 6: 18-24.

Gangeskar, R., 2002. Ocean current estimated from X-band radar sea surface, images. IEEE. Trans. Geosci. Remote Sens., 40: 783-792.

Huang, W. and E. Gill, 2012. Surface current measurement under low sea state using dual polarized X-band nautical radar. IEEE. J. Sel. Top. Appl. Earth Obs. Remote Sens., 5: 1868-1873.

Komen, G.J., L. Cavaleri and M. Donelan, 1996. Dynamics and Modelling of Ocean Waves. Cambridge University Press, Cambridge, UK., ISBN-13:978-0-521-47047-6, Pages: 531.

Reddy, N.G.K. and N. Manoharan, 2014. Ship recycling: An important mile stone for India. Indian J. Sci. Technol., 7: 15-21.

Senet, C.M., J. Seemann and F. Ziemer, 2001. The near-surface current velocity determined from image sequences of the sea surface. IEEE. Trans. Geosci. Remote Sens., 39: 492-505.

Sethuramalingam, T.K. and B. Nagaraj, 2015. A soft computing approach on ship trajectory control for marine applications. ARPN. J. Eng. Appl. Sci., 10: 4281-4286.

Shen, C., W. Huang and E.W. Gill, 2014. An alternative method for surface current extraction from X-band marine radar images. Proceedings of the 2014 IEEE International Symposium on Geoscience and Remote Sensing, July 13-18, 2014, IEEE, Québec, Canada, ISBN:978-1-4799-5775-0, pp: 4370-4373.

Tukey, J.W., 1967. An introduction to the calculations of numerical spectrum analysis. Spectral Anal. Time Ser., Vol. 25,

Veerakumar, P., M. Dheepak and S.V. Saravanan, 2017. PLC based automatic control for onboard ship gangway conveyor system. Intl. J. Mech. Eng. Technol., 8: 229-235.

Young, I.R., W. Rosenthal and F. Ziemer, 1985. A three-dimensional analysis of marine radar images for the determination of ocean wave directionality and surface currents. J. Geophys. Res. Oceans, 90: 1049-1059.